

# Electromechanical Breakdown Mechanism of Passive Film in Alternating Current-Related Corrosion of Carbon Steel Under Cathodic Protection Condition

A. Brenna,<sup>‡,\*</sup> M. Ormellese,<sup>\*</sup> and L. Lazzari<sup>\*</sup>

Submitted for publication: September 19, 2015. Revised and accepted: April 22, 2016. Preprint

available online: April 22, 2016, <http://dx.doi.org/10.5006/1849>.

<sup>‡</sup>Corresponding author. E-mail: [andrea.brenna@polimi.it](mailto:andrea.brenna@polimi.it).

<sup>\*</sup>Politecnico di Milano – Dipartimento di Chimica, Materiali e Ingegneria Chimica “Giulio Natta”, Via Mancinelli, 7 – 20131 Milano, Italy.

## Abstract

Buried carbon steel pipe are provided with corrosion prevention systems, namely an insulating coating and a cathodic protection system which reduces (or halts) corrosion rate as a result of soil corrosiveness. The presence of alternating current (AC) interference may cause serious corrosion damages on metallic structures corresponding to coating defects, even if the  $-0.850 V_{CSE}$  protection criterion is matched. Nowadays, the AC corrosion mechanism, as well as the protection criteria in the presence of AC, is still controversial and debated. In this paper, a two-step AC corrosion mechanism of carbon steel under cathodic protection condition is proposed: (1) AC causes the electromechanical breakdown of the passive film formed on carbon steel under overprotection condition, and (2) after passive film breakdown, high-pH chemical corrosion takes place. In order to investigate AC effects on passive condition (Step 1), experimental tests have been performed on stainless steels in neutral solution, as a result of its passive behavior: AC has harmful effects on passive condition, reducing anodic overpotential, and causing film breakdown over a critical AC interference level. The electromechanical oxide breakdown mechanism resulting from high alternating electric fields (of the order of  $10^6$  V/cm) within the passive film is proposed. Electrostriction stresses are a possible explanation. After film breakdown, corrosion can occur if the pH inside the crack is close to 14; this strong alkalization can be reached in overprotection condition (high cathodic current density) and in the presence of AC.

**Key Words:** alternating current (AC), carbon steel, cathodic protection, passivity, pH changes and effects, stainless steels

## 1. INTRODUCTION

Carbon steel pipe used to transport hydrocarbons and dangerous fluids are provided with corrosion prevention systems, namely an insulating coating and a cathodic protection (CP) system which reduces corrosion rate below 10  $\mu\text{m}/\text{y}$ , which is the maximum acceptable corrosion rate fixed by CP standard.<sup>1</sup> Carbon steel in aerated soil operates in protection condition if the IR-free potential (not affected by ohmic drop) is more negative than  $-0.850\text{ V}$  vs. CSE (Cu/CuSO<sub>4</sub> reference electrode,  $+0.318\text{ V}$  vs. standard hydrogen electrode [SHE]).<sup>1-2</sup> Alternating current (AC)-induced corrosion still represents a serious threat to the integrity of underground structures even if CP is properly applied. When a metallic pipeline is parallel to an AC source (typically, high-voltage overhead or underground power lines or AC traction systems), AC interference can take place by a conductive or inductive mechanism, causing corrosion corresponding to coating defects or porosity where metal is exposed to soil corrosiveness. There is agreement that at the utility frequencies (50 Hz or 60 Hz), AC causes corrosion at much higher current density than direct current (DC) stray current, as also confirmed by a previous work.<sup>3</sup> In the last 30 y, several theories have been proposed to describe the mechanism by which AC produces and enhances corrosion of carbon steel.<sup>3-15</sup> Nevertheless, the corrosion mechanism, as well as the protection criteria,<sup>16-20</sup> in the presence of AC is still controversial and debated.

In this work, a proposed AC-induced corrosion mechanism of carbon steel under CP condition is discussed. The model takes into account previous results obtained in the first phase of the research during which the effects of AC interference on kinetics parameters (anodic and cathodic polarization curves) and on corrosion rate were widely investigated in various environments (e.g., soil-simulating solution, artificial seawater) for different metals (carbon steel, galvanized steel, zinc, and copper). A “mixed corrosion mechanism” was initially hypothesized, with a general decrease of both anodic and cathodic overpotentials and an increase of exchange current density.<sup>3,7</sup>

In the last years, an extensive effort in Europe has been performed to provide acceptable criteria to evaluate AC corrosion likelihood. The European standard EN 15280<sup>21</sup> (“Evaluation of AC Corrosion Likelihood of Buried Pipelines—Application to Cathodically Protected Pipelines”) reports that in the presence of AC interference the criteria given in EN 12954<sup>1</sup> are not sufficient to demonstrate that steel is protected against corrosion, and provides acceptable levels, measurements and mitigation procedures, and information to deal with AC-induced corrosion likelihood.

According to the acceptable interference levels reported by EN 15280,<sup>21</sup> as a first step the AC voltage on the pipeline (measured as an average over a representative period of time, e.g., 24 h) should be decreased to 15 V R.M.S. or less. Then, AC corrosion mitigation can be achieved by complying with criteria defined in EN 12954,<sup>1</sup> and: (1) by maintaining AC density ( $j_{\text{AC}}$ ) lower than 30 A/m<sup>2</sup> on a 1 cm<sup>2</sup> coupon or probe; (2) by maintaining average cathodic current density ( $j_{\text{DC}}$ ) lower than 1 A/m<sup>2</sup> if AC density is more than

30 A/m<sup>2</sup>; or (3) by maintaining the ratio between AC density and DC density ( $j_{AC}/j_{DC}$ ) of less than 3 over a representative period of time (e.g., 24 h).

In other words, while no AC density restrictions are defined for DC densities lower than 1 A/m<sup>2</sup>, AC density is restricted to values lower than 30 A/m<sup>2</sup> with DC density in the range from 1 A/m<sup>2</sup> to 10 A/m<sup>2</sup>, which corresponds to overprotection condition (potential more negative than  $-1.2 V_{CSE}$ ). It follows that AC corrosion of buried steel structures does not depend only on the AC interference level (expressed by AC voltage or AC density), but also on the CP condition of the pipe, i.e., AC corrosion likelihood increases as DC density increases.

More severe acceptable interference levels were defined by means of preliminary long-term CP tests (described in detail in a previous work<sup>22</sup>) in the presence of AC stationary interference on carbon steel specimens Type L360<sup>23</sup> in soil-simulating conditions, i.e., sand saturated with a sulfate and chloride ions containing solution. Laboratory tests showed that in overprotection condition, i.e., potential more negative than  $-1.2 V_{CSE}$ , only a few A/m<sup>2</sup> of AC density (in the range 5 to 20) can cause corrosion of overprotected carbon steel. Results showed that cathodic current densities lower than 1 A/m<sup>2</sup> in combination with AC density higher than 30 A/m<sup>2</sup> can lead to AC corrosion, as well as DC density higher than 1 A/m<sup>2</sup> in combination with AC density higher than 10 A/m<sup>2</sup>.

In order to understand the mechanism by which AC causes corrosion of overprotected carbon steel, some preliminary thermodynamic considerations are mandatory. From a thermodynamic point of view, CP of carbon steel in soil is defined as the establishment of a state of immunity (or quasi-immunity) by a cathodic polarization which halts (or reduces) steel corrosion rate. Nevertheless, over time the pH of the electrolyte at the metal-to-soil interface will increase as a result of the cathodic reactions (i.e., oxygen reduction and hydrogen evolution at more negative potential) occurring on the metal surface. As hydroxyl ions production is regulated by the cathodic current supplied to the metal, the local pH will be greater corresponding to high CP levels, i.e., high cathodic current or more negative potentials (overprotection condition). On the other hand, the presence of transport processes as a result of a concentration gradient and of electrophoretic migration contributes to establish a pH profile in close proximity to the metal surface. The pH increase identifies a thermodynamic condition defined by the chemically-induced formation of a passive film of Fe<sub>2</sub>O<sub>3</sub> and Fe<sub>3</sub>O<sub>4</sub>, according to the Pourbaix's diagram of the iron-water system at 298 K<sup>24</sup> and in agreement with Pourbaix,<sup>11</sup> who reports that local alkalization via CP is beneficial because of the formation of a "perfectly protective passive film." Freiman, et al.,<sup>25</sup> outlined the concept of "cathodic passivation" strictly promoted by the potential-pH condition. In soil and in stagnant solution, where the transport and diffusion of chemical species and oxygen is slow, the pH close to the metal surface increases with cathodic current density, reaching a considerably higher level (11 to

12) than in bulk aqueous solutions. The effects of electrolyte alkalization under CP condition are well known in seawater CP application, where the alkalization promotes the growth on steel surface of a calcium carbonate and magnesium hydroxide scale, which acts as a natural protective layer. CP effectiveness on carbon steel does not seem to be related only to the potential lowering to an immunity condition but also to the formation of a protective passive film promoted by the alkalization of the metal-to-solution interface (*chemical effect* of CP<sup>2</sup>).

According to this premise, in order to investigate the effect of AC on passive condition, tailored tests (i.e., potentiodynamic tests and alternating breakdown voltage measurement) have been performed on stainless steel in neutral solution. Undoubtedly, the passive film formed on stainless steel is different in composition and structure to that formed on carbon steel at alkaline pH under CP condition. Nevertheless, in this work an investigation of harmful effects of AC on passive films is discussed, proposing an analogy between the breakdown of the passive film of stainless steel in neutral solution and carbon steel under CP condition. Although some AC corrosion models recognize possible harmful effects of AC on passive condition, none provide a description of the mechanism by which AC corrodes passive metals. For instance, Nielsen, et al.,<sup>9</sup> report that AC-induced potential oscillations between the passive, the immunity, and the high-pH corrosion domains of the iron Pourbaix diagram may cause corrosion by a destabilization of the passive layer. Similarly, Pourbaix<sup>11</sup> state that nonprotective films can form when the potential oscillates between the passivation domain and the immunity domain, and that superimposed AC can destroy passivation films that would be perfectly protective in the absence of AC.

## **2. EXPERIMENTAL PROCEDURES**

### **2.1 *Potentiodynamic Tests on Stainless Steel in the Presence of Alternating Current Interference***

Anodic and cathodic potentiodynamic tests were performed on Type X5CrNiMo 17-12-2 stainless steel (Type 316, UNS S31600<sup>(1)</sup>, EN 1.4401<sup>26</sup>) in the presence of AC stationary interference. After preparation and cleaning operations according to ASTM Standard G1,<sup>27</sup> stainless steel specimens were placed in a PTFE cylindrical sample holder (Figure 1) made of two watertight caps. A circular area of 1 cm<sup>2</sup> of the metal was exposed to the electrolyte. A metal rod was screwed in a hole on the top of the sample holder to provide the electrical contact with the specimen inside the cap. In order to prevent the contact between the metal rod and the surrounding environment, a glass tube was placed around the screw and was pressed against the sample holder interposing a polymeric gasket.

---

<sup>(1)</sup> UNS numbers are listed in *Metals and Alloys in the Unified Numbering System*, published by the Society of Automotive Engineers (SAE International) and cosponsored by ASTM International.

Specimens were placed in a test cell containing 1 L aerated stagnant solution (exposed to atmosphere) containing 500 mg/L chlorides. Bulk temperature was kept constant at 20°C ( $\pm 2^\circ\text{C}$ ). A four-electrode test cell configuration was adopted (Figure 2): in addition to the working (W) and the reference electrode (RE) (Ag/AgCl<sub>KCl,sat.</sub>, +0.2 V<sub>SHE</sub>), two MMO-Ti (mixed-metal oxides titanium) counter electrodes were used to supply the polarization (CE<sub>CP</sub>) and the interference (CE<sub>AC</sub>) currents by means of a proper electrical circuit designed in order to separate the DC and AC signals (Figure 2). AC was limited to approximately 1% of the total AC by a 20 H inductance in the DC mesh, while DC was halted by a 500  $\mu\text{F}$  capacitor in the AC mesh.<sup>7</sup>

After 1 h conditioning in free corrosion condition until a stable potential was reached, AC interference was applied by means of an AC feeder (variac device). The circulating AC was measured by interposing a digital amperometer connected in series to the circuit. Three AC densities were applied in a stationary way: 10, 30, and 50 A/m<sup>2</sup> (50 Hz frequency), such that the electrical charge for unit area (given by the product between AC density and time) supplied to the metal was constant. In order to minimize the ohmic drop in the solution between the reference and the working electrode, a Luggin glass capillary was used. Potentiodynamic polarization was performed from -1.2 V vs. Ag/AgCl<sub>KCl,sat.</sub> to 0.4 V vs. Ag/AgCl<sub>KCl,sat.</sub> with a potential scan rate of 0.17 mV/s according to standard.<sup>28</sup> Because of experimental restrictions with the electrical equipment, in the presence of AC, potentiodynamic testing was not performed in a continuous mode (continuous displacement of potential) but by steps, varying the potential of 10 mV every 60 s, respecting the same potential scan rate.

## 2.2 *Alternating Voltage Measurements*

Alternating voltage measurements were performed on Type X5CrNi 18-10 (Type 304, UNS S30400, EN 1.4301<sup>26</sup>) and Type 316 (EN 1.4401<sup>26</sup>) stainless steels in free corrosion condition and on cathodically protected carbon steel specimens Type L360.<sup>23</sup> CP was applied in a potentiostatic control at three overprotection potentials: -1.1, -1.2, and -1.3 V<sub>CSE</sub>. Specimens were prepared according to the procedure described previously and placed in a test cell filled with 1 L of a stagnant and aerated solution containing 500 mg/L of sulfate ions. No chlorides were added to the solution. After 1 h conditioning, AC was applied by means of an AC feeder and a MMO-Ti counter electrode. AC was applied after attainment of a steady value of the protection current density. The stable value of DC current density at the tested polarization potentials was 0.22, 0.58, and 1.25 A/m<sup>2</sup>, respectively. The alternating voltage was increased by steps

(about 10 mV every min) and measured by an external high-impedance voltmeter with respect to an Ag/AgCl<sub>KCl,sat.</sub> reference electrode placed in a Luggin glass capillary whose tip was positioned in close proximity to the metal surface (estimated distance: 1 mm). The circulating current was measured by means of a digital amperometer in series to the circuit. Simultaneously, DC potential was measured with respect to the reference electrode in the Luggin capillary which allows elimination of the ohmic drop contribution in the measurement (resulting from the circulating current in the solution path between the sample and the reference electrode). Three tests for each material were performed.

### 3. RESULTS

#### 3.1 *Potentiodynamic Tests on Stainless Steel in the Presence of Alternating Current Interference*

Potentiodynamic tests were performed on Type 316 stainless steel in order to investigate the effect of AC interference on passive condition, i.e., on anodic and cathodic potential-current curves. Preliminary results showed that AC interference up to 50 A/m<sup>2</sup> causes a weakening of the passive film formed on stainless steel resulting in the decrease of the critical chlorides threshold for pitting corrosion initiation.<sup>29</sup> Figure 3 shows potentiodynamic curves (E-log j) in the presence of 10, 30, and 50 A/m<sup>2</sup> AC density. A control curve in the absence of AC interference is reported for comparison. The passive region is well defined in the control curve: the metal is in passive condition and corrosion current is equal to the passive current density, namely in the range 3 mA/m<sup>2</sup> to 5 mA/m<sup>2</sup>, which corresponds to a penetration rate of about 5 μm/y, i.e., corrosion is negligible. AC has a detrimental effect on passive condition, with the decrease of anodic overpotential and the weakening of the passive film. Corrosion current density in the presence of AC can be estimated by the intersection of anodic and cathodic curves, which identifies the working point of the electrochemical system. Corrosion current density was lower than 10 mA/m<sup>2</sup> only in the presence of 10 A/m<sup>2</sup> AC density. AC of 50 A/m<sup>2</sup> causes a corrosion rate of about 100 μm/y, more than one order of magnitude greater than corrosion rate in the control condition. A minor effect is observed considering the cathodic branch of the polarization curve (oxygen limiting current density and hydrogen evolution overpotential). Oxygen limiting current density is in the range 200 mA/m<sup>2</sup> to 300 mA/m<sup>2</sup> in stagnant condition, regardless the magnitude of the overlapped AC. Potentiodynamic tests confirm the effect of AC on anodic overpotentials, already observed for active and active-passive metals in different exposure conditions.<sup>7,30</sup>

#### 3.2 *Alternating Voltage Measurements*

*Tests on Stainless Steels in Neutral Solution—*

Figure 4 shows AC density and DC potential ( $E_{\text{corr}}$ ) as a function of the applied alternating voltage ( $V_{\text{AC}}$ ) on Type 304 stainless steel. Three tests were performed to guarantee test repeatability. AC density increased as the applied voltage increased, as expected. The experimental curve can be divided in two sections as a result of a strong increase of the curve slope (i.e., more current is exchanged corresponding to a voltage increase). Corrosion potential moves initially to more positive values in the presence of AC and then, corresponding to the slope variation of the  $j_{\text{AC}}-V_{\text{AC}}$  curve, a drop of corrosion potential is measured. The potential drop could be associated to the formation of active (corroding) area corresponding to the attainment of a critical voltage (in the following breakdown alternating voltage,  $V_{\text{BD}}$ ), with subsequent corrosion of the substrate and an increase of the circulating current in the electrical circuit. The average  $V_{\text{BD}}$  is 0.27 V for Type 304 stainless steel, corresponding to about 20 A/m<sup>2</sup> AC density (Table 1).

Figure 5 shows AC density and potential as a function of the alternating voltage on Type 316 stainless steel specimens. The same considerations discussed previously could be extended: AC density increases by increasing the applied voltage, until the attainment of the breakdown alternating voltage ( $V_{\text{BD}}$ ). Corresponding to the slope-variation of the curve, DC potential decreases as a result of the formation of a macrocell between active and passive area. As reported in Table 2, mean value of  $V_{\text{BD}}$  is 0.32 V and the corresponding AC density is about 23 A/m<sup>2</sup>, both greater than the values measured for Type 304 stainless steel.

#### *Tests on Carbon Steel Under Cathodic Protection Condition—*

Alternating voltage measurements were performed on carbon steel specimens cathodically polarized in a potentiostatic control at fixed overprotection potentials:  $-1.1$ ,  $-1.2$ , and  $-1.3$   $V_{\text{CSE}}$ , the most critical according to AC corrosion.<sup>21-22</sup> Figure 6 shows AC density as a function of the applied voltage. The breakdown voltage (and the corresponding AC density) was calculated corresponding to the intersection point between the tangent of the first part of the curve and the tangent of the second part after passive film breakdown.  $V_{\text{BD}}$  increased as the protection potential became more negative, i.e., from 0.05 V at  $-1.1$   $V_{\text{CSE}}$  to 0.18 V at  $-1.3$   $V_{\text{CSE}}$ , while the corresponding AC density decreased as the DC current density increased (Table 3).

## 4. DISCUSSION

### 4.1 *Alternating Current Corrosion Mechanism*

A two-step AC corrosion mechanism of carbon steel under CP condition is proposed:

- (a) *Step 1*: AC causes the electromechanical breakdown of the passive film formed on cathodically protected carbon steel surface;
- (b) *Step 2*: after passive film breakdown, high-pH chemical corrosion occurs in overprotection condition.

### 4.2 *Step 1: The Passive Film Electromechanical Breakdown Mechanism*

The electromechanical film breakdown mechanism is unique considering the interpretation of AC corrosion phenomenon but is well known in the study of localized corrosion, as in the description of pitting phenomena. Generally, the theoretical models that describe the initiation process of passive film breakdown may be grouped into three classes:<sup>31-34</sup> (1) adsorption-induced mechanism, where the adsorption of aggressive ions as chlorides is of major importance; (2) ion migration and penetration models; and (3) mechanical film breakdown theories.

The adsorption and penetration models are strictly related to the presence of aggressive anions, such as chloride ions in pitting corrosion, in the electrolyte in contact with the passive metal. The adsorption mechanism for pits nucleation starts with the formation of surface complexes that are transferred to the electrolyte much faster than uncomplexed iron ions (e.g., halides enhance the transfer of  $\text{Fe}^{3+}$  and  $\text{Ni}^{2+}$  from the oxide to the electrolyte). This leads to a local thinning of the passive layer and finally to its complete breakdown and the formation of a pit. The penetration mechanism requires transfer of the aggressive anions through the passive layer to the metal/oxide interface, where they cause internal stresses and pit nucleation. The latter model, proposed first by Vetter and Strehblow<sup>35</sup> and Sato<sup>36</sup> requires the film mechanical cracking resulting from a sudden change of the electrode potential; the resulting crack gives direct access for the aggressive ions to the unprotected metal. Taking into account the thermodynamic description provided by Sato,<sup>36</sup> stresses in oxide films can arise from the interfacial tension in the film, electrostriction pressure resulting from the presence of a high electric field, internal stresses caused by the different properties of the metal and the film, or the presence of impurities. Using a thermodynamic framework, Sato suggested that the mechanical failure of the film can result from high electromechanical stresses (electrostriction pressure) generated by the presence of an electric field across the film and by the interfacial tension, which is not negligible as a result of the thin thickness of the oxide. Generally, electrostriction is defined as the deformation of a dielectric material as the result of the

applied electric field, which polarizes the randomly aligned electrical domains within the material; hence, the opposite sides of the domains become differently charged and attract each other, reducing material thickness in the direction of the applied field. It is possible to consider the simplest polarization model of a dielectric oxide layer in the presence of a constant electric field. The system consists of a dielectric film of thickness  $L$  mechanically free to deform on the electrolyte side but constrained on the metal surface. The film pressure  $\sigma$  (N/m<sup>2</sup>) acts perpendicular to the film and is determined by the atmospheric pressure ( $\sigma_0$ ), the electrostriction pressure ( $\sigma_E$ ) resulting from the presence of the electric field ( $E$ ), and the interfacial tension ( $\sigma_\gamma$ ):<sup>36</sup>

$$\sigma = \sigma_0 + \sigma_E + \sigma_\gamma = \sigma_0 + \frac{\epsilon_0(\epsilon_R - 1)E^2}{8\pi} - \frac{\gamma}{L} \quad (1)$$

where  $\epsilon_0$  is vacuum electric permittivity and  $\epsilon_R$  is relative permittivity of the oxide, which is related to the dipole moment per unit volume of the film. The electrostriction pressure ( $\sigma_E$ ) depends on the electric properties of the film (by means of  $\epsilon_R$ ) and on the square of the electric field. The interfacial effect is high at low film thickness and decreases as the film thickness increases, i.e., film pressure ( $\sigma$ ) tends to the electrostriction pressure, increasing the thickness of the film.

Passive film breakdown occurs when the induced stress reaches the film mechanical resistance ( $\sigma_R$ ), corresponding to the breakdown electric field ( $E_{BD}$ ):

$$E_{BD} = \sqrt{\frac{\left(\sigma_R - \sigma_0 + \frac{\gamma}{L}\right) \times 8\pi}{\epsilon_0(\epsilon_R - 1)}} \quad (2)$$

The breakdown electric field decreases as the dielectric constant of the oxide increases, resulting from the larger polarization of the domains of the passive film and, as expected, by decreasing the mechanical properties of the oxide, expressed by  $\sigma_R$ . As Sato<sup>36</sup> and Strehblow<sup>32</sup> reported, metal oxides or hydroxide in the presence of electric field of the order of 10<sup>6</sup> V/cm could deform or break mechanically because of the high electrostriction pressure.

Sato's model refers to a simplified approach of passive film electrostriction which takes into account the response of a simple parallel plate capacitor polarized by the external electric field until its breakdown. More accurate models<sup>37-39</sup> were proposed in order to investigate the electromechanical behavior of anodic

oxide film taking into account the semi-conductive properties of passive films. Nevertheless, even though there is a difference in some assumptions, these models establish a correlation between the occurrence of the breakdown phenomena of the passive film and the mechanical stresses induced by the presence of an electric field.

Alternating voltage measurements were performed on passive metals in order to ascertain the presence of a breakdown alternating voltage ( $V_{BD}$ ) above which passive film breakdown occurs (expected to be in the order of  $10^6$  V/cm). The alternating voltage measured according to the procedure described is the sum of three contributions:

$$V_{AC} = V_{AC,solution} + V_{AC,oxide} + V_{AC,metal} \quad (3)$$

where  $V_{AC,solution}$  is the voltage drop in the solution between the tip of the Luggin capillary and the specimen,  $V_{AC,oxide}$  is the voltage contribution across the passive film, and  $V_{AC,metal}$  is the contribution in the metallic phase (specimen and electric cables).  $V_{AC,solution}$  is generally the sum of the ohmic drop in the electrolyte and all of the contributions localized at the interface between the metal and the solution, related to the capacitive and resistive impedances of the electrochemical double layer. While the voltage drop in the metallic phase ( $V_{AC,metal}$ ) can be reasonably neglected, it may be too restrictive to extend this assumption to the voltage between the oxide and the tip of the Luggin capillary ( $V_{AC,solution}$ ). Nevertheless, a first set of experimental tests were performed considering both  $V_{AC,metal}$  and  $V_{AC,solution}$  negligible. The measurement provides only an estimation of the alternating electric field ( $E$ ) across the passive film, given by the ratio between the alternating voltage between the opposite sides of the oxide and the thickness ( $L$ ) of the passive film:

$$E = \frac{V_{AC,oxide}}{L} \cong \frac{V_{AC}}{L} \quad (4)$$

The breakdown electric field,  $E_{BD}$ , in Equation (2) is then defined as the breakdown alternating voltage measured experimentally ( $V_{BD}$ ) for unit passive film thickness. A passive film thickness of 1 nm is assumed for calculation, according to values reported in the specific literature.<sup>33-34,40</sup>

#### *Tests on Stainless Steels in Neutral Solution—*

Breakdown electric fields for Type 304 (Pitting Resistance Equivalent Number [PRE<sub>N</sub>] equal to 18) and Type 316 (PRE<sub>N</sub> index 25) stainless steels are reported in Tables 1 and 2. Breakdown electric

field is of the order of  $10^6$  V/cm, in agreement with theoretical prediction provided by the electrostriction model. Experimental tests confirm the existence of an electromechanical breakdown mechanism of the passive film in the presence of AC. Furthermore, the breakdown alternating electric field increases as the corrosion resistance of the passive film increases: considering a film thickness of 1 nm, the breakdown electric field increases from  $2.7 \times 10^6$  V/cm to  $3.2 \times 10^6$  V/cm as the  $PRE_N$  index of stainless steel increases from 18 to 25. In conclusion, potential oscillations resulting from the superimposed AC may cause electromechanical stresses in the passive film, which depend on the electric properties of the film and on the electric field.

#### *Tests on Carbon Steel Under Cathodic Protection Condition—*

Table 3 reports breakdown alternating voltages measured on carbon steel specimens cathodically polarized at fixed overprotection potentials:  $-1.1$ ,  $-1.2$ , and  $-1.3$  V<sub>CSE</sub>. While the breakdown electric field increases as the potential becomes more negative, from  $0.5 \times 10^6$  V/cm to  $1.8 \times 10^6$  V/cm, the corresponding AC density and the  $j_{AC}/j_{DC}$  ratio decrease, as the protection current density increases. The critical current densities ratio ( $j_{AC}/j_{DC}$ ) depends on the protection potential, i.e., it decreases as the protection potential becomes more negative, according to practical experience and to CP criteria discussed in a previous work.<sup>22</sup> It is reasonable to suppose that this response is a result of the electric properties (or thickness) of the passive film formed at different polarization potential. Furthermore, the localized morphology of AC-induced corrosion suggests the achievement of a critical breakdown condition corresponding to “weak points” of the passive film (as defects, presence of impurities, lower thickness zones) or disuniformities in AC distribution on the metal surface.

### **4.3 Step 2: High-pH Corrosion of Overprotected Carbon Steel**

After passive film breakdown, corrosion can occur only if thermodynamically possible and, in the absence of stray currents, corrosion of cathodically protected steel does not occur. The thermodynamic Pourbaix diagram of the iron-water system<sup>24</sup> shows two corrosion domains, corresponding to neutral and acid environments with formation of ferrous and ferric ions (at low and high potential, respectively) and to high-pH condition at potentials considered safe for carbon steel cathodically protected. As reported by Pourbaix in his work,<sup>24</sup> two equilibrium iron-water system diagrams can be established, depending on the stability of  $Fe_3O_4$  and  $Fe_2O_3$  or  $Fe(OH)_2$  and  $Fe(OH)_3$ , respectively.

Considering  $Fe(OH)_2$  and  $Fe(OH)_3$  as solid substances, the high-pH corrosion domain is delimited by a vertical equilibrium line on the potential-pH diagram, which means that the corrosion reaction is

potential-independent and occurs over a threshold value of pH. In equilibrium condition, the pH threshold is close to 14 and corrosion occurs with the formation of green dihypoferrite ions ( $\text{HFeO}_2^-$ ). According to the proposed mechanism, after the electromechanical breakdown of the passive film on steel under CP condition, corrosion can occur only if the potential-pH condition of the interfered metal crosses the high-pH corrosion domain.

Galvanostatic tests were performed in order to measure the pH profile in the test solution in contact with a carbon steel specimen Type L360 under CP condition. pH profiles are reported in a previous work<sup>29</sup> and show that a strong alkalization occurs close to the metal under CP condition corresponding to high cathodic current densities. In the presence of current densities higher than  $5 \text{ A/m}^2$ , the measured pH in the stagnant soil-simulating solution in close proximity to the metal surface is in the range between 13 and 14, albeit the local pH depends on several factors, such as chemical composition, presence of electric fields, diffusion processes, corrosion reactions, and electrolyte convective properties.

As in pitting corrosion, the local environment in contact with the metal becomes more important than the bulk environment and should be considered in order to investigate the “true” corrosion condition. In pitting corrosion, the macrocell current exchanged between the pit and the surrounding area causes chloride ions migration and a strong acidification within the pit. As reported by Pourbaix,<sup>41</sup> a cathodic treatment of pitted steel leads to the pH increase of the solution inside cracks or pits, which becomes progressively neutral and then alkaline, resulting in a noncorrosive solution. Similarly, after the passive film cracking resulting from AC interference, the local solution inside the crack may become more aggressive with respect to the bulk electrolyte, as a result of the local pH increase (up to 14) in overprotection condition. In other words, high cathodic current density could cause a strong alkalization in the crack, making chemical corrosion possible.

Moreover, the electrical charge equilibrium should be considered. In cathodic protection, electrons are involved in the cathodic process, which depends on the potential assumed by the metal. Thus, below the equilibrium potential, the applied cathodic current makes electrons available to the metal; therefore, no anodic reactions can take place. Consequently, if no oxidation reaction takes place, such as iron ion production, this can occur only through *chemical corrosion*, which is not potential dependent, or, in other words, is not influenced by the electrons made available otherwise.

As electrons are not involved in the corrosion reaction, the process is controlled by a chemical equilibrium between species, instead of electrochemical. Chemical corrosion is well known, for instance for aluminum, to which corrosion is thermodynamically possible at low and high pH (amphoteric behavior) with formation of  $\text{Al}^{3+}$  and aluminate  $\text{AlO}_2^-$  ions, respectively. The dissolution process of aluminum oxide is potential-independent and occurs below (at low pH) and over (at high pH) critical pH

thresholds. Accordingly, in the presence of chlorides, CP of aluminum cannot be achieved by bringing the metal potential in the immunity domain that would be at potentials as negative as about  $-2.3 V_{CSE}$  because the strong alkalization causes aluminum corrosion even if a cathodic current is applied, as a result of the main role played by pH on chemical dissolution reaction. Likewise, chemical corrosion of carbon steel under CP condition in the presence of AC could be hypothesized in the cracks of the passive film. If chemical corrosion occurs, a further cathodic current supply to the metal could be harmful, resulting from the pH increase. Therefore, overprotection (high cathodic current density) is the most dangerous condition in the presence of AC and must be avoided.

## 5. CONCLUSIONS

Experimental tests on carbon steel specimens under cathodic protection condition showed that in the presence of AC interference corrosion can occur, even if the  $-0.850 V_{CSE}$  criterion is matched. A two-step AC corrosion mechanism is proposed. In the first step, AC causes the electromechanical breakdown of the passive film formed on carbon steel under CP condition. Electrostriction appears to be a good explanation of the passive film breakdown mechanism, as a result of the presence of high alternating electric field (of the order of  $10^6 V/cm$ ) across the passive film. After film breakdown, high-pH chemical corrosion occurs in overprotection condition as a result of the high CP current density supplied to the metal.

## 6. REFERENCES

1. EN 12954:2001, "Cathodic Protection of Buried or Immersed Metallic Structures - General Principles and Application for Pipelines" (Brussels, Belgium: European Committee for Standardization [CEN], 2001).
2. L. Lazzari, P. Pedferri, *Cathodic Protection* (Milan, Italy: Polipress, 2006), p. 365.
3. S. Goidanich, L. Lazzari, M. Ormellese, *Corros. Sci.* 52 (2010): p. 916-922.
4. L.Y. Xu, X. Su, Y.F. Cheng, *Corros. Sci.* 66 (2013): p. 263-268.
5. M. Büchler, *Mater. Corros.* 63, 12 (2012): p. 1181-1187.
6. A.Q. Fu, Y.F. Cheng, *Can. Metall. Quart.* 51, 1 (2012): p. 81-90.
7. S. Goidanich, L. Lazzari, M. Ormellese, *Corros. Sci.* 52 (2010): p. 491-497.
8. H. Xiao, S.B. Lalvani, *J. Electrochem. Soc.* 155, 2 (2008): p. 69-74.
9. L.V. Nielsen, "AC Corrosion," in *Oil and Gas Pipelines: Integrity and Safety Handbook*, ed. R.W. Revie (Hoboken, NJ: John Wiley & Sons, Inc., 2015), p. 363-385.

10. D.Z. Tang, Y.X. Du, M.X. Lu, Z.T. Jiang, L. Dong, J.J. Wang, *Mater. Corros.* 66, 3 (2015): p. 278-285.
11. A. Pourbaix, *MP* 39, 3 (2000): p. 34-37.
12. D.K. Kim, S. Muralidharan, T.H. Ha, J.H. Bae, Y.C. Ha, H.G. Lee, J.D. Scantlebury, *Electrochim. Acta* 51, 25 (2006): p. 5259-5267.
13. Y. Hosokawa, F. Kajiyama, T. Fukuoka, *Corrosion* 60, 4 (2004): p. 408-413.
14. S.B. Lalvani, X. Lin, *Corros. Sci.* 38, 10 (1996): p. 1709-1719.
15. U. Bertocci, *Corrosion* 35, 5 (1979): p. 211-215.
16. X. He, G. Jiang, Y. Qiu, G. Zhang, X. Jin, Z. Xiang, Z. Zhang, H. Tang, *Mater. Corros.* 63, 6 (2012): p. 534-543.
17. I. Ibrahim, M. Meyer, H. Takenouti, B. Tribollet, *J. Brazilian Chem. Soc.* 27, 3 (2016): p. 605-615.
18. F. Kajiyama, Y. Nakamura, *Corrosion* 55, 2 (1999): p. 200-205.
19. M. Büchler, H.G. Schöneich, *Corrosion* 65, 9 (2009): p. 578-586.
20. Y. Hosokawa, F. Kajiyama, Y. Nakamura, *Corrosion* 60, 3 (2004): p. 304-312.
21. EN 15280:2013, "Evaluation of AC Corrosion Likelihood of Buried Pipelines Applicable to Cathodically Protected Pipelines" (Brussels, Belgium: European Committee for Standardization [CEN], 2013).
22. A. Brenna, L. Lazzari, M. Pedferri, M. Ormellese, *Metall. Italiana* 6 (2014): p. 29-34.
23. EN ISO 3183:2012, "Petroleum and Natural Gas Industries - Steel Pipe for Pipeline Transportation Systems" (Brussels, Belgium: European Committee for Iron and Steel Standardization [ECISS], 2012).
24. M. Pourbaix, *Atlas of Electrochemical Equilibria in Aqueous Solutions* (Houston, TX: NACE International, 1974), p. 644.
25. L.I. Freiman, E.G. Kuznetsova, *Prot. Met.* 37, 5 (2001): p. 484-490.
26. EN 10088-1:2014, "Stainless Steels - Part 1: List of Stainless Steels" (Brussels, Belgium: European Committee for Iron and Steel Standardization [ECISS], 2014).
27. ASTM G1-03, "Standard Practice for Preparing, Cleaning, and Evaluating Corrosion Test Specimens" (West Conshohocken, PA: ASTM International, 2011).
28. EN ISO 17475:2008, "Corrosion of Metals and Alloys - Electrochemical Test Methods - Guidelines for Conducting Potentiostatic and Potentiodynamic Polarization Measurements" (Brussels, Belgium: European Committee for Standardization [CEN], 2008).
29. A. Brenna, M.V. Diamanti, L. Lazzari, M. Ormellese, "A Proposal of AC Corrosion Mechanism in Cathodic Protection," Tech. Proc. of NSTI Nanotechnology Conference and Expo (Danville, CA: Nano Science and Technology Institute, 2011), p. 4.

30. J.L. Wendt, D.-T. Chin, *Corros. Sci.* 25, 10 (1985): p. 889-900.
31. H. Böhni, "Localized Corrosion of Passive Metals," in *Uhlig's Corrosion Handbook*, ed. R. Winston Revie, 3rd ed. (Hoboken, NJ: John Wiley & Sons, Inc., 2011), p. 157-169.
32. H.-H. Strehblow, "Mechanism of Pitting Corrosion," in *Corrosion Mechanisms in Theory and Practice*, ed. P. Marcus, 2nd ed., revised and expanded (New York, NY: Marcel Dekker, Inc., 2002), p. 243-285.
33. G.T. Burstein, "Passivity and Localized Corrosion," in *Shreir's Corrosion*, ed. T.J.A. Richardson, vol. 2, Corrosion in Liquids (Amsterdam, Netherlands: Elsevier B.V., 2010), p. 731-752.
34. Z. Szklarska Smialowska, *Pitting Corrosion of Metals* (Houston, TX: NACE, 1986), p. 417.
35. K.J. Vetter, H.-H. Strehblow, *J. Pharma. Sci. Math.* 74, 10 (1970): p. 1024-1035.
36. N. Sato, *Electrochim. Acta* 16, 10 (1971): p. 1683-1692.
37. Z. Szklarska-Smialowska, *Corros. Sci.* 44, 5 (2002): p. 1143-1149.
38. J-F. Vanhumbecq, J. Proost, *Electrochim. Acta* 53 (2008): p. 6165-6172.
39. Y. Tang, R. Ballarini, *J. Mech. Phys. Solids* 59 (2011): p. 178-193.
40. F.P. Fehlner, M.J. Graham, "Thin Oxide Film Formation on Metals," in *Corrosion Mechanisms in Theory and Practice*, ed. P. Marcus, 2nd ed., revised and expanded (New York, NY: Marcel Dekker, Inc., 2002), p. 171-187.
41. M. Pourbaix, *Lectures on Electrochemical Corrosion* (Houston, TX: NACE, 1995), p. 644.

#### Figure Captions:

Figure 1. Carbon steel and stainless steel specimen configuration.

Figure 2. Two-mesh AC-DC electrical circuit for potentiodynamic tests in the presence of AC.

Figure 3. Type 316 stainless steel: potentiodynamic anodic and cathodic polarization curves in the presence of AC stationary interference at 20°C ( $\pm 2^\circ\text{C}$ ).

Figure 4. Type 304 stainless steel: AC density ( $j_{AC}$ ) and corrosion potential ( $E_{corr}$ ) varying the applied alternating voltage ( $V_{AC}$ ).

Figure 5. Type 316 stainless steel: AC density ( $j_{AC}$ ) and corrosion potential ( $E_{corr}$ ) varying the applied alternating voltage ( $V_{AC}$ ).

Figure 6. AC density ( $j_{AC}$ ) varying the applied alternating voltage ( $V_{AC}$ ) and protection potential of carbon steel specimens under cathodic protection condition.

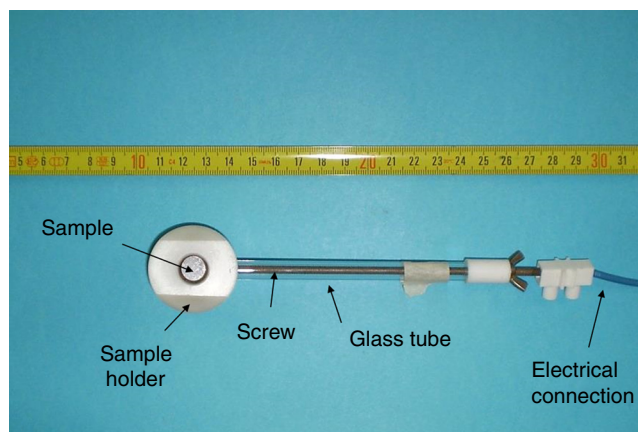


FIGURE 1.

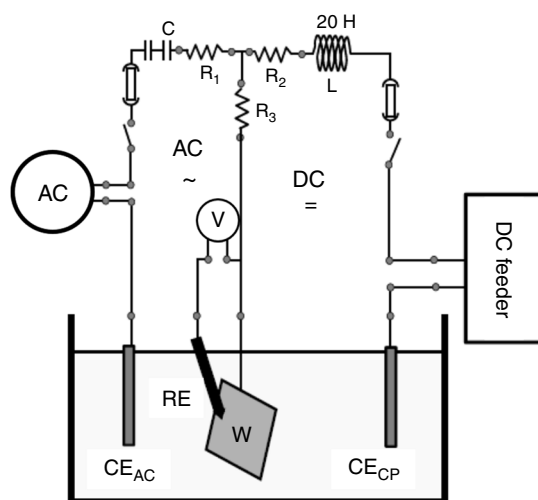


FIGURE 2.

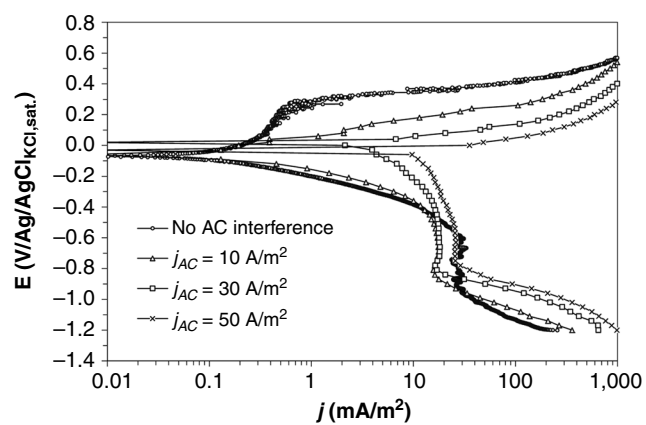


FIGURE 3.

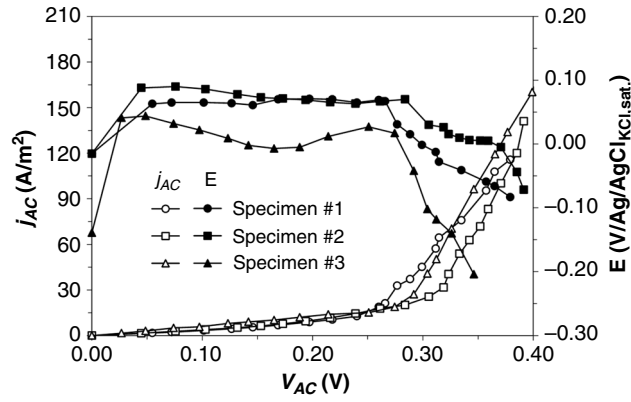


FIGURE 4.

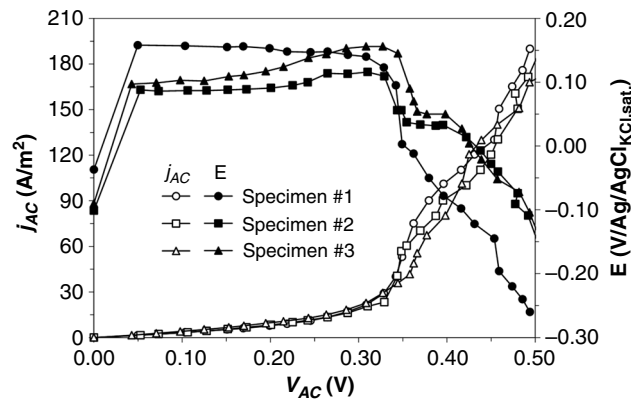


FIGURE 5.

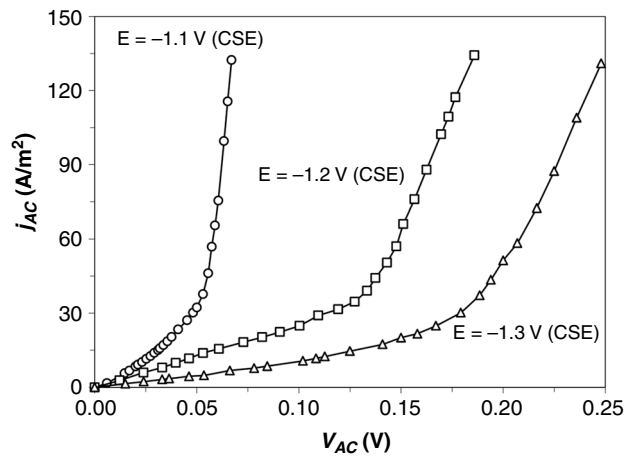


FIGURE 6.

**Table 1** Breakdown Alternating Voltage ( $V_{BD}$ ) and Calculated Electric Field Assuming 1 nm Passive Film Thickness for Type 304 Stainless Steel

Type 304 (X5CrNi 18-10) Specimen	Breakdown Alternating Voltage ( $V_{BD}$ , V)	AC Density ( $j_{AC}$ , A/m <sup>2</sup> )	Breakdown Electric Field (1 nm film thickness, $\times 10^6$ V/cm)
1	0.27	21	2.7
2	0.28	20	2.8
3	0.27	19	2.7
Mean	0.27	20	2.7

**Table 2** Breakdown Alternating Voltage ( $V_{BD}$ ) and Calculated Electric Field Assuming 1 nm Passive Film Thickness for Type 316 Stainless Steel

Type 316 (X5CrNiMo 17-12-2) Specimen	Breakdown Alternating Voltage ( $V_{BD}$ , V)	AC Density ( $j_{AC}$ , A/m <sup>2</sup> )	Breakdown Electric Field (1 nm film thickness, $\times 10^6$ V/cm)
1	0.31	22	3.1
2	0.33	23	3.3
3	0.31	23	3.1
Mean	0.32	23	3.2

**Table 3** Breakdown Alternating Voltage ( $V_{BD}$ ) and Calculated Electric Field Assuming 1 nm Passive Film Thickness for Carbon Steel Under Cathodic Protection Condition

<b>E (<math>V_{CSE}</math>)</b>	<b>DC Density (<math>j_{DC}</math>, A/m<sup>2</sup>)</b>	<b>AC Density (<math>j_{AC}</math>, A/m<sup>2</sup>)</b>	<b><math>j_{AC}/j_{DC}</math></b>	<b>Breakdown Alternating Voltage (<math>V_{BD}</math>, V)</b>	<b>Breakdown Electric Field (1 nm film thickness, <math>\times 10^6</math> V/cm)</b>
-1.1	0.22	31	139	0.05	0.5
-1.2	0.58	37	64	0.14	1.4
-1.3	1.25	24	19	0.18	1.8